Experimental modeling of dry friction coefficient between steel and aluminum alloy in the condition of severe plastic deformation

Aşırı plastik deformasyon koşulunda çelik ve alüminyum alaşımı arasındaki kuru sürtünme katsayısının deneysel modellenmesi

Amir Sharifi Miavaghi[1], Haleh Kangarlou[2]

[1]Department of Physics, Urmia University of Technology, Urmia, Iran
[2]Department of Physics, Islamic Azad University, Faculty of Science, Urmia Branch, Iran

ARTICLE INFO

ABSTRACT

Through with current study the friction coefficient values for steel-aluminum alloy system in high contact pressures and low speed conditions have been obtained. To aim this goal a new arrangement of friction test apparatus which already was offered in literature has been fabricated. Towards, the effects of surface roughness and applied normal load on friction coefficient have been investigated. The results clearly revealed that friction coefficient is significantly influenced by applied normal load and reduces with increasing in load. Furthermore, surface roughness influences friction coefficient; but its effect is not as important as applied normal load. Finally, the suggested theoretical friction models in literature are compared with an experimental model of this study.

Keywords: Experimental modeling, Contact pressures, Friction coefficient, Severe plastic deformation, Coulomb's law

ÖZET

Bu çalışma ile, yüksek temas basınçları ve düşük hız koşullarında çelik alüminyum alaşım sistemi için sürtünme katsayısı değerleri elde edilmiştir. Bu amaca yönelik olarak, daha önce literatürde sunulan sürtünme test cihazlarının yeni bir düzenlemesi yapılmış, yüzey pürüzlülüğünün ve uygulanan normal yükün sürtünme katsayısı üzerindeki etkileri araştırılmıştır. Sonuçlar açıkça göstermektedir ki, sürtünme katsayısı, uygulanan normal yükten oldukça etkilenmekte ve yük arttıkça azalmaktadır. Ayrıca, yüzey pürüzlülüğü sürtünme katsayısını da etkilemektedir. Ancak etkisi, uygulanan normal yük kadar önemli değildir. Son olarak literatürde önerilen teorik sürtünme modelleri, bu çalışmanın deneysel modeli ile karşılaştırılmıştır.

Anahtar sözcükler: Deneysel modelleme, Temas basınçları, Katsayı değeri, Aşırı plastik deformasyon, Coulomb yasası

1. Introduction

Friction is not a material property; but it is a characteristic of a system including base and sliding materials, surface treatment and working conditions. It is proved that friction coefficient is considerably influenced by temperature, sliding velocity, normal pressure, surface roughness, etc (1-3). Hence a friction coefficient of pair of materials at low contact pressures cannot be suitable to use in a system with a very high contact pressures.

Despite, there are few researches dedicated to find a friction coefficient via simulation, experimental methods are still the only reliable way for measuring friction coefficient values (4). Indeed, friction coefficient is critical in order to calculate a required force for the forming of materials and also achieving accurate results from modeling using numerical methods.

For emprically measurment of friction coefficient values, considering a real working condition of the

system, many tribometer devices have been designed and are in use by the researchers. Severe plastic deformation is a special process which involves very high contact pressures (about the several order of the sample's yield strength) (5) and in this process the friction plays the most important role on a magnetude of the required force (6). However, for many material pairs there are no reliable friction coefficient values in litreture (7). Researchers have developed a friction test apparatus for measuring friction coefficient between sheet metals in a crash test (8). They have designed their device to be used in measurement of friction coefficient values at a relatively high contact pressures (up to 100 MPa). However, this amount of pressure is still too low with respect to pressures which are involved in some metal forming methods like a severe plastic deformation process. Recently, investigators suggested a suitable means for measuring friction coefficient values at very high contact pressures and low speeds (9). However, their suggested tribometer have some shortcomings that will be addressed in this study. In current study the apparatus suggested by researchers is redesigned. Among all materials, Aluminum-7075 is an attractive in metal forming process and many researchers are investigating various aspects of processing Aluminum-7075 by Severe Plastic Deformation methods. But the frictional behavior of Aluminum -7075 when contacting with a steel die has not been investigated extensively. Then, in current investigation as a case study the Aluminum Alloy-Steel system is chosen to measure its friction coefficient in different pressures to show the capabilities of the new design of tribometer. In addition, the effect of surface roughness and applied load on a friction coefficient will be investigated. The experimental model which is offered in this study for friction coefficient values in Aluminum Alloy-Steel system can be used in Severe Plastic Deformation calculations. In addition, this experimental model can be useful to validate predictive models available in literature for coefficient of friction. An example of such comparison is offered.
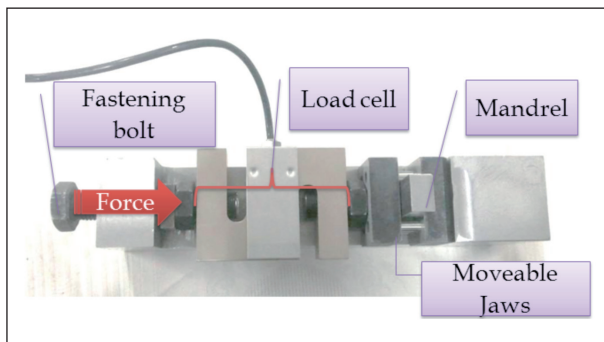
2. Experimental Setup

The main mechanism of the experimental setup is the same with one reported in reference (9). A photograph of a tribometer fabricated for this study is shown in Figure 1. It consists of the main body, Mandrel, two jaws and a load cell for measuring an applied force. Material type of the jaws is chosen as the common material type of the real Severe Plastic Deformation process. It was steel in our experiment. The Mandrel holds a sample and moves it between two jaws. In order to guarantee that only sample tips will be in contact with jaws' surface, the specimen length is prepared about 0.1 millimeter longer than the Mandrel wide length on each side (Figure 2).

One of the jaws can move easily in one direction which helps to locate a mandrel and specimen between two jaws, but its motion is limited in other directions by four guide rods. A moveable jaw can be pushed by a load cell that itself is connected to a fastening screw. By tightening a screw, it is possible to create compression stress at the specimen between two jaws and inside a Mandrel. A whole system is attached to a tensile test machine as shown in Figure 3. In fact, the plunger of the tensile test machine is connected to the Mandrel of the tribometer. An indicator shows an applied load in a load cell and a specimen. After setting a desired applied hydrostatic load on a specimen by fastening a screw and checking the load in an indicator, the plunger of a tensile test machine moves the specimen down on a jaws face. Displacement speed of the plunger can be controlled via computer. Also, the load and displacement values of the plunger are recorded by an electronic data acquisition system which is available on a machine.

This system is a new arrangement of a friction test apparatus which already offered by other researchers (9). However, the current design has three main differences with the tribometer offered in reference. Firstly, here load cell is used in order to measure the applied force
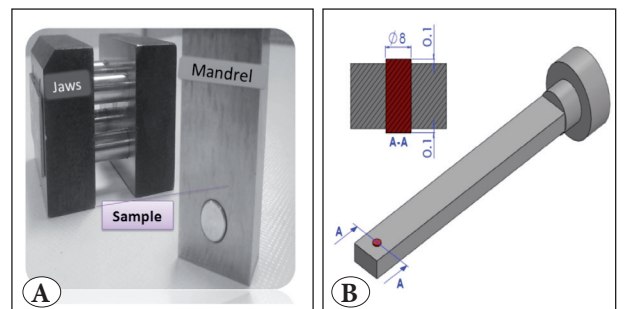

Figure 1: A tribometer of this study.

Figure 2: (A) a photo of Jaws, Mandrel and a sample, **(B)** schematic of the Mandrel and a sample on it.

that is easier and mostly more precise than strain gauges on connecting screws. Secondly, at the design of reference tribometer, two guide rods hardly can assure the parallelism of the jaws, especially due to the sample tips motion. Therefore here, four guide rods are used to constrain the Jaw's in all directions except sliding direction and finally, the mechanism of applied force changed here, whereas now it is possible to apply load by turning just one nut instead of two nuts in the design of reference design.

3. Experimental Procedure

Jaws were made from AISI 4340 steel (with yield strength of 710 MPa). Their surface was hardened to about 60 Rockwell C. Specimens were made of 7075 aluminum alloy with yield strenght of about 550 MPa and their shear strength of about 300 MPa. Stress-strain curve of 7075 aluminum alloy which is used in this study has been represented in Figure 4. Specimens had 15.2 mm length and 8mm diameter. Special care has been taken in order to ensure the parallelism of the sample tips using special fixtures. In addition, two sets of specimens were prepared with two different surface treatments (polished and machined surfaces). Specimens are located in a Mandrel hole with transition fit. After the Mandrel with a sample inside of it is moved to the center point of the Jaws, the moveable jaws is fastened by turning a screw. The sample is fully confined inside the Mandrel and then, by fastening a screw it is produced a hydrostatic pressure on a sample which is followed by a very low speed motion of

the plunger. Hence, the condition of the friction in Severe Plastic Deformation methods is satisfying in current friction coefficient measuring system. In order to study the effect of normal pressure on a friction coefficient, an applied force adjusted in a way to squeezes the specimen with 50, 100, 200, 300, 400, 500, 600 and 700 MPa normal pressures for different test samples. During each test, the next step was applying a tangential force on a contact region between the sample and jaws via Mandrel (or the tensile test machine) in order to slide a specimen on a Jaw's face. A total sliding of the samples was 1 mm for all tests that is done with a tangential rate of 1 mm per minute (which is close to normal velocities in Severe Plastic Deformation process). As previously mentioned, the sliding force system (tensile test machine) was connected to a data acquisition system with the capability of recording 100 data per second. The recorded data was displacement of a specimen on a Jaw's face and a required force for this sliding. Whole test was accomplished for both polished and machined samples in order to study the effect of surface preparation in different normal load regimes.

4. Results and Discussion

The force-displacement curves of the experimental tests for polished and machined samples are shown in Figure 5 and 6, respectively. In order to check the repeatability of the results, all tests are repeated twice. Stick-slip phenomena were dominant during all tests. This fact can also be understood from saw type force-displacement curves (Figure 5,6). During a friction test, a drop of the apparent normal pressure was observed. It was varied from 3% to 10% for different normal pressures that was readable from load cell indicator. Tests are performed under displacement controlled loading conditions. As it
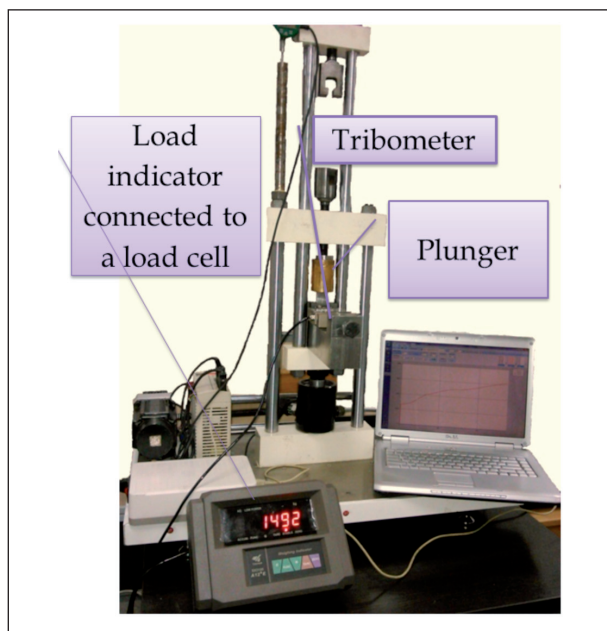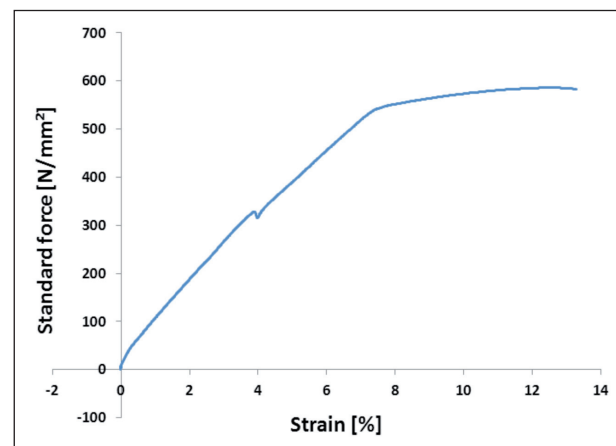
Figure 3: Shows an experimental setup.

Figure 4: Represents stress-strain curve of 7075 aluminum alloy.

can be found from Figures 5 and 6, force-displacement curves consists of two distinguished stages: in the first stage the sample still resists against sliding and the reported displacements (by increasing force) is related to the elastic deformation of the system (test machine and asperities). This stage can be assumed linear. The second stage can be referred to sliding of the sample on Jaws' surface. This stage starts just after the tangential force overcomes static frictional resistance of the system. This point can be used to calculate the static friction coefficient of the system using Eq.1. In this equation, μ stands for a friction coefficient, F_T, is a tangential force and F_N, shows normal force. It should be noted that the factor 2 in equation (1) is due to the presence of two sliding surfaces.

$$\mu = \frac{F_T}{2F_N} \qquad (1)$$

As it can be found from Figure 5, static friction forces in lower loads (lower than 400 MPa) are obviously higher than the following stationary kinetic friction forces. This is caused by the fact that with a higher initial load the asperities of contacting parts are already flattened mildly in microscopic scale (and surface roughness changes), this may cause a reduction in plowing component of the initial friction. This is in agreement with the results of Molecular Dynamic simulation(10). Then, it can be concluded that both initial topography of the surfaces and the magnitude of initial applied load is important in determination of static friction coefficient.

The total coefficient of friction is composed of two components; the adhesion component and the plowing component. The plowing component depends on the degree of plastic deformation taking place at the asperity level, while adhesion component depends on the material pair and lubrication and also on surface roughness. An adhesion component of friction decreases with increasing in surface roughness. The reason for this is that by increasing in roughness, the average distance between the molecules of two sliding components increases and the secondary atomic forces are weakening. In this study in order to study the effect of surface roughness on friction value, two sets of samples with different surface roughness have been tested. In Figure 7 it compared static friction values for polished and machined surfaces. The effect of surface roughness on friction coefficient can be explained by its effect on real area of contact. By increasing in real area of contact the number of contacting asperities increases as well and hence the plow component of the friction growths dependently. In addition, increscent in real area of contact increases the total atomic forces between two surfaces and thus, the adhesion component of the friction increases.

The effect of surface roughness on the real area of contact has been studied by many researchers (11). According to results of an empirical study, there is considerable difference between the real areas of contact of surfaces with different roughness for all normal pressures (12). This fact is reflected in a little difference in coefficient of friction of two sample sets with different
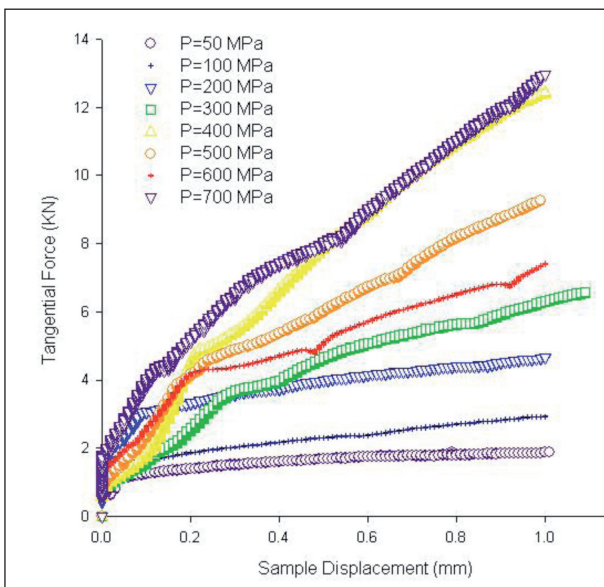

Figure 5: Shows sample displacement versus tangential force for polished samples.
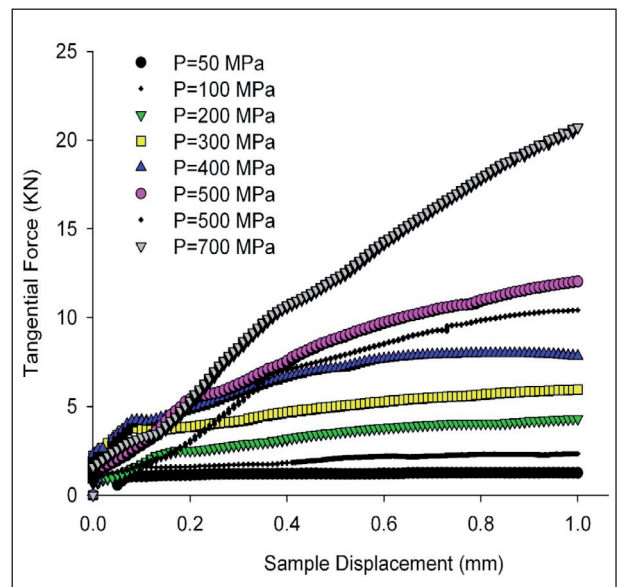

Figure 6: Shows sample displacement versus tangential force for machined samples.

surface roughness in Figure 7. Looking Figure 7, it seems that the effect of surface roughness is considerable in lower loads.

In this study, a kinetic friction coefficient is calculated again using Eq. 1. However, for kinetic friction, there is variable stationary coefficient with sliding distance; hence it averaged over all F_T from sliding point to the end of the curve and used this F_{Tave} to calculate an averaged kinetic friction coefficient of the system. Figure 8 shows a kinetic friction coefficient values for polished and machined samples. Although, the surface roughness of machined and polished samples do not differ so much, however, according to Figures 7 and 8 it can simply be concluded that the effect of normal pressure is much greater than surface roughness for the range of study. Like the static friction coefficient, the effect of surface roughness is significant just in lower normal pressures (lower than softer material yield strength) and the friction coefficient goes to be independent of surface roughness in higher normal pressures.

In addition, researches show that the rate of increscent in real area of contact due to increscent in normal load is higher for smooth surfaces (13). Then, no surprising that as it is clear from Figure 8 a friction coefficient of polished samples in experiments is more sensitive to changes in normal load. Where, the difference between the maximum and minimum coefficient of friction for the range of study is higher for polished samples. The surface roughness properties for samples after the test are measured for testing with 600 MPa pressure. The results showed that there is no meaningful change in surface roughness before and after the friction test for samples of this study.

5. Comparison of the Theoretical and Experimental Models

At the following, in order to show another application of the experimental model offered through with Figure 7, the amount of agreement of the proposed theoretical models in literature with the experimental model of the current study is investigated. Three suggested models which are chosen for comparison are including Amonton's model, shear friction model and a model in reference (14).

5.1. Comparison with Amonton's Friction Model

Amonton's friction model (Eq. 2) quantifies interface friction by lumping all of the interface phenomena into a non-dimensional friction coefficient (μ).

$$\tau_f = \mu P_a \qquad (2)$$

Where, P_a stands for apparent normal pressure and τ_f is the frictional shear strength of the interference. In Amonton's friction model, it assumed that friction coefficient to be constant. This is true for the most of engineering problems. But, in many metal forming processes, the interface pressure, P, changes drastically during the process and can reach a multiple of the yield strength of the material. Thus, the linear relationship between τ_f and P, as described by Eq. 2, cannot be valid at high contact pressure levels. This is because in this equation, there is no limit for the right hand of the equation, but the left hand (a shear stress, τ_f), cannot exceed the maximum shear strength, *k*, of the deformed work piece material. Therefore, the coefficient of friction becomes meaningless when μP_a exceeds τ_f.
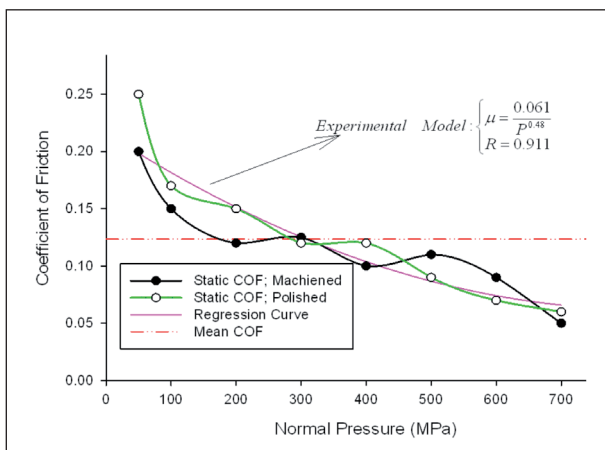

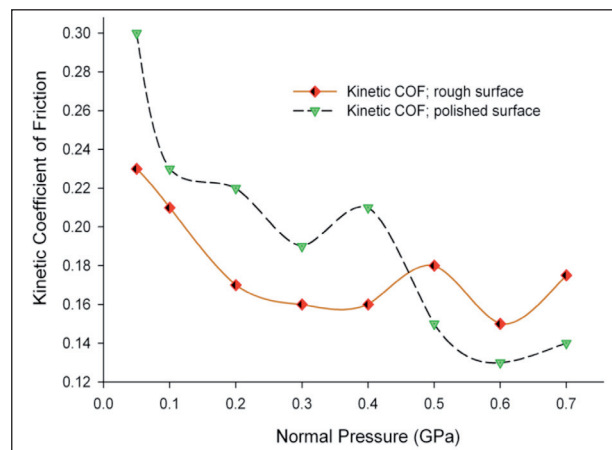**Figure 7:** Comparison of static friction coefficient in polished and machined samples.

Figure 8: Shows comparison of kinetic friction coefficient in polished and as turned surface roughness.

According to data reported by several researchers a simplified relationship between real area of contact and an applied load may be defined as equation (3) (15, 16):

$$\frac{A_{real}}{A_a} = \alpha P_a + b = 0.0013 P_a + 0.16 \qquad (3)$$

Where A_{real} indicates real area of contact, A_a, shows an apparent area of contact and is a parameter which depends on plasticity index (ψ) of the contact system (17). Then one may conclude that α parameter accompany the effect of material type and surface roughness. By substituting Eq. 3 in Eq. 1 (Amonton's law), one can obtain:

$$\mu = \frac{F_T}{F_N} = \frac{\tau_f}{P_a}\frac{A_{real}}{A_a} = \frac{\tau_f}{P_a}(0.0013 P_a + 0.16)$$
$$= (0.0013 + \frac{0.16}{P_a})\tau_f \qquad (4)$$

According to above discussion, Eq. 4 is practically valid only to pressures lower than about 700 MPa (as per Eq. 3, the relation $\frac{A_{real}}{A_a}$ cannot exceeds one). This finding is in good agreement with the finding of literature (16). According to Eq. 4, coefficient of friction has a direct relation with interfacial stiffness (τ_f) and at a same time has a revers relation with apparent normal pressure. However, as it is shown at the top-right side of Figure 7, experimental model of the current work reveals that a coefficient of friction has a relation with the inverse of the square of normal pressure. The theoretical and experimental models are compared in Figure 9. According to Figure 9, Amonton's friction model is capable of predicting coefficient of friction in higher

normal loads. But the predictions based on Amonton's friction model are not enough accurate in lower loads.

5.2. Comparison with Shear Friction Model

To avoid limitations of Amonton-Coulomb's model, the shear friction model (Eq. 5) has been proposed (18):

$$\tau_f = m\frac{\bar{\sigma}}{\sqrt{3}} = m\left(\frac{A_{real}}{A_a}\right).k \qquad (5)$$

In this equation, *m* is the shear factor which is the function of a real area of contact ratio and equals to zero for no friction, and to unity for a sticking friction condition. Sticking friction condition happens where the sliding at the interface is preempted by shearing of the base material (19). Example of the sticking friction condition is in High Pressure Torsion (HPT) process; where the magnitude of hydrostatic pressure exceeds several Gigabytes. It should be noted that a shear factor, *m,* is a function of real contact area and dependently a function of an applied normal load. Generally, According to shear friction model the friction stress, τ_f, at low pressures is proportional to the normal pressure (Amonton's law) and at high pressures is equal to the yield stress in pure shear. In Eq. 5, the maximum frictional shear stress (τ_f) will be equal to the maximum shear strength at the interface (*k*) only at the condition of full contact of sliding surfaces which normally happens in very high contact pressures where the contact ratio limits unity (Eq. 3).

According to experimental results and considering strain hardening, the value of τ_f for aluminum 7075 is about 360MPa. Then, with a simple calculation, one can found that according to shear model the maximum frictional force of 17.6 KN is anticipated for samples of this study. But as it is clear from Figures 5 & 6 static frictional force for samples of the current study is much lower than 17.6 KN. Then the shear model cannot acceptably anticipate the frictional shear value at the interface of aluminum alloy and steel (also see Figure 9).

5.3. Comparison with Model of Reference (14)

Another semi-analytical model for coefficient of friction is offered in reference (14):

$$\mu = (0.26 + \frac{0.43}{\psi})\frac{P^{0.0095\psi}}{P^{0.09}} \qquad (6)$$

Where, ψ, is the plasticity index. If a rational value for plasticity index between steel and aluminum alloy assumed to be 3; then the Eq. 6 will be as:
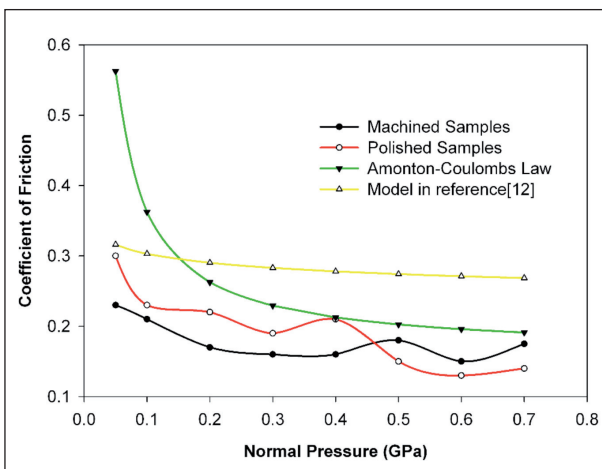

Figure 9: Comparison between suggested models for coefficient of friction in literature and experimental results.

$$\mu = \frac{0.403}{P^{0.062}} \qquad (7)$$

As it is obvious from Figure 9, the model of reference (12) (Eq. 7) also cannot good estimate the relation between normal pressure and coefficient of friction at the interface of steel and aluminum alloy for all pressure ranges. This model is acceptably predicts the friction coefficient in low contact pressures.

It can be concluded that the suggested models for friction at high contact pressures are useful in qualitative analysis, but need drastic revision in order to be capable in predicting frictional shear at the interface of the steel and aluminum alloy.

6. Conclusion

A revised version of friction test apparatus has been presented. It is more accurate and flexible than a test machine introduced in references for doing experiments under high contact pressures and low speed conditions. The experimental model of the friction coefficient values for steel-aluminum alloy system at a low sliding regime and different contact pressures have been obtained which is useful in Severe Plastic Deformation analysis. The effect of normal pressure and surface roughness on the value of coefficient of friction is empirically investigated. The results show that the effect of normal pressure is much greater than surface roughness. For a constant surface roughness either static or kinetic friction coefficient values show exponential reduction by increasing in applied load but plateaued at higher normal pressures. In addition, it found that the effect of surface roughness is considerable just in contact pressures lower than material yield strength. In higher contact pressures surface roughness has not sizeable effect on friction coefficient. The comparison of results for the experimental model offered here with the suggested theoretical models in literature show that, none of theoretical models for friction coefficient cannot good estimate the coefficient of friction, quantitatively and all need a drastic revision to be acceptable in predicting frictional shear at the interface of material pairs.

References

1. Ulutan, M., et al., (2010). Effect of Different Surface Treatment Methods on the Friction and Wear Behavior of AISI 4140 Steel. 26(3), 251-257.

2. K.M. Adel, A.S. Dhia, and M.J. Ghazali, (2009). the effect of laser surface hardening on the wear and friction characteristics of acicular bainitic ductile iron. 4(2), 5.

3. Johnson, K. and R. Cameron, (1967). Fourth paper: shear behaviour of elastohydrodynamic oil films at high rolling contact pressures. 182(1), 307-330.

4. Patil, B., U. Chakkingal, and P. Kumar, (2008). influence of friction in equal channel angular pressing – a study with simulation. 5(13-15.

5. Eskandarzade, M., Masoumi, A., Faraji, Gh., Mohammadpour, M., Sabrina Yan, X, (2017). A new designed incremental high pressure torsion process for producing long nanostructured rod samples. 695, 1539-1546.

6. Eskandarzade, M., Masoumi, A., Faraji,. Gh. (2017) Numrical and analytical investigation of an ultrasonic assisted ECAP process. 2(2), 166-183.

7. Mehdi Eskandarzade, A.M., Ghader Faraji, (2016). Numerical and analytical investigation of an ultrasonic assisted ECAP process. 2(2), 18.

8. Lai, X., et al., (2012). An experimental method for characterizing friction properties of sheet metal under high contact pressure. 289(0), 82-94.

9. Pougis, A., et al., (2013). Dry friction of steel under high pressure in quasi-static conditions. 67(0), 27-35.

10. Spijker, P., G. Anciaux, and J.-F. Molinari, (2011). Dry sliding contact between rough surfaces at the atomistic scale. 44(2), 279-285.

11. Greenwood, J. and J. Tripp, (1970). The contact of two nominally flat rough surfaces. 185(1), 625-633.

12. Greenwood, J.A. and J.H. Tripp, (1967). The elastic contact of rough spheres. 34(1), 153-159.

13. Dwyer-Joyce, R., B. Drinkwater, and A. Quinn, (2001). The use of ultrasound in the investigation of rough surface interfaces. 123(1), 8-16.

14. Cohen, D., Y. Kligerman, and I. Etsion, (2008). A model for contact and static friction of nominally flat rough surfaces under full stick contact condition. 130(3), 031401.

15. Eguchi, M., T. Shibamiya, and T. Yamamoto, (2009). Measurement of real contact area and analysis of stick/slip region. 42(11), 1781-1791.

16. Buchner, B., M. Buchner, and B. Buchmayr, (2009). Determination of the real contact area for numerical simulation. 42(6), 897-901.

17. Li, L., I. Etsion, and F. Talke, (2010). Contact area and static friction of rough surfaces with high plasticity index. 132(3), 031401.

18. Pal, A.K., (1973). A study of metallic friction phenomena with high normal pressure. 26(2), 261-272.

19. Kim, H. and N. Kardes, (2012). Friction and lubrication.